7-2016

Diquark Mass Differences from Unquenched Lattice QCD

Yujiang Bi
Wuhan University, China

Hao Cai
Wuhan University, China

Ying Chen
Chinese Academy of Sciences, China

Ming Gong
Chinese Academy of Sciences, China

Zhaofeng Liu
University of Kentucky

See next page for additional authors

Chinese Physics C

PARTICLES AND FIELDS • OPEN ACCESS

Diquark mass differences from unquenched lattice QCD

Diquark mass differences from unquenched lattice QCD *

Yujiang Bi(毕玉江)[1;1)] Hao Cai(蔡浩)[1;2)] Ying Chen(陈莹)[2] Ming Gong(宫明)[2]
Zhaofeng Liu(刘朝峰)[2;3)] Hao-Xue Qiao(乔豪学)[1] Yi-Bo Yang(杨一玻)[3]

[1] School of Physics and Technology, Wuhan University, Wuhan 430072, China
[2] Institute of High Energy Physics and Theoretical Physics Center for Science Facilities, Chinese Academy of Sciences, Beijing 100049, China
[3] Department of Physics and Astronomy, University of Kentucky, Lexington, KY 40506, USA

Abstract: We calculate diquark correlation functions in the Landau gauge on the lattice using overlap valence quarks and 2+1-flavor domain wall fermion configurations. Quark masses are extracted from the scalar part of quark propagators in the Landau gauge. The scalar diquark quark mass difference and axial vector scalar diquark mass difference are obtained for diquarks composed of two light quarks and of a strange and a light quark. The light sea quark mass dependence of the results is examined. Two lattice spacings are used to check the discretization effects. The coarse and fine lattices are of sizes $24^3\times64$ and $32^3\times64$ with inverse spacings $1/a=1.75(4)$ GeV and 2.33(5) GeV, respectively.

Keywords: lattice QCD, diquarks, overlap fermions, Landau gauge

PACS: 11.15.Ha, 12.38.-t, 12.38.Gc **DOI:** 10.1088/1674-1137/40/7/073106

1 Introduction

Diquarks were introduced a long time ago and are used in many phenomenology studies of strong interactions. For example, diquarks are used to describe baryons with a quark-diquark picture for explaining the missing states [1]. They are also used to explain the $\Delta I=1/2$ rule in weak nonleptonic decays [2, 3]. A review on diquarks is given in Ref. [1]. Since the discovery of the X(3872) by the Belle Collaboration [4], experiments have observed many so-called XYZ states [5]. It is difficult to interpret these states as conventional heavy quarkonia. Molecules and tetraquarks are proposed to explain some of these quarkonium-like states. In the tetraquark scenario, a diquark and an antidiquark form a four quark state.

Quantum Chromodynamics (QCD) is the theory describing the strong interaction among quarks and gluons, from which the properties of diquark correlations (if any) should be understood. At low energies, QCD has to be solved by nonperturbative methods since the strong coupling constant becomes so strong that perturbative calculations break down. In this work we study diquarks starting from the QCD action by using lattice QCD simulations. Diquarks have been studied on the lattice from various approaches [6–12] to deal with the fact that they are not color singlets. Diquark masses were also calculated in QCD sum rules, see, for example, Refs. [13, 14]. The stability of diquarks has also been discussed [15].

The scalar diquark is supposed to be the state with the strongest correlation. The mass difference between diquarks with various quantum numbers can reflect the relative size of the correlation. In Ref. [16], the scalar diquark and quark mass difference as well as the axial vector and scalar diquark mass difference are estimated from baryon spectroscopy. On the lattice, diquark mass and mass differences can be studied in a fixed gauge. So far, the masses and mass differences are calculated mostly in the quenched approximation on the lattice. Here we calculate them by using 2+1 flavor domain wall fermion configurations. For the valence quark, we use overlap fermions. Previous lattice calculations focused

Received 27 October 2015, Revised 4 March 2016

∗ Supported by National Science Foundation of China (11575197, 10835002, 11405178, 11335001), joint funds of NSFC (U1232109), MG and ZL are partially supported by the Youth Innovation Promotion Association of CAS (2015013, 2011013), YC and ZL acknowledge support of NSFC and DFG (CRC110)

1) E-mail: biyujiang@ihep.ac.cn
2) E-mail: hcai@whu.edu.cn
3) E-mail: liuzf@ihep.ac.cn

on diquarks composed of the light up and down quarks. In this work we consider diquarks composed of a strange and a light quark as well as of two light quarks.

Diquark correlations are induced by spin dependent interactions. Thus they become weaker as the masses of the quarks increase. We can look into the mass dependence of diquark correlations by varying the current quark masses on the lattice.

Our results for diquark mass differences and diquark quark mass differences are summaried in Table 14. In general they agree with the estimations in Ref. [16]. The exception is the scalar diquark and strange quark mass difference for diquarks composed of a strange and a light quark. Our result for this difference is smaller than the estimation in Ref. [16].

The paper is organized as follows. In Section 2, we present the details of our calculation. The results and discussion are given in Section 3. Finally we summarize in Section 4.

2 Correlation functions and lattice setup

The two quarks in the scalar diquark ($J^P = 0^+$) in the color antitriplet representation are attractive to each other as favored by perturbative one gluon exchange [17] and by instanton interactions [18, 19]. It is often called a "good" diquark. The next favored diquark is the axial vector diquark ($J^P = 1^+$) and it is called a "bad" diquark. The other diquarks with $J^P = 0^-, 1^-$ are supposed to be even more energetic and therefore their masses are higher. The diquarks in the color sextet representation have much larger color electrostatic field energy and are not favored by various models [16].

Therefore we focus on the color antitriplet diquarks and calculate their masses on the lattice. The interpolating operators used in this work for diquarks with various quantum numbers are given in Table 1, where C is the charge conjugation operator. In the operators q_1 and q_2 are u and $d(s)$ respectively.

Table 1. Interpolating fields and correlation functions of diquarks. A trace is performed in color space.

J^P (diquark)	operators	correlators
0^+(good)	$J_c^5 = \epsilon_{abc}[q_1^a C\gamma_5 q_2^b]$	$\sum_{\vec{x}} \langle \Omega \vert T J_c^5(x) \bar{J}_c^5(0) \vert \Omega \rangle$
0^+(good)	$J_c^{05} = \epsilon_{abc}[q_1^a C\gamma_0\gamma_5 q_2^b]$	$\sum_{\vec{x}} \langle \Omega \vert T J_c^{05}(x) \bar{J}_c^{05}(0) \vert \Omega \rangle$
1^+(bad)	$J_c^i = \epsilon_{abc}[q_1^a C\gamma_i q_2^b]$	$\frac{1}{3}\sum_i \sum_{\vec{x}} \langle \Omega \vert T J_c^i(x) \bar{J}_c^i(0) \vert \Omega \rangle$
1^+(bad)	$J_c = \epsilon_{abc}[q_1^a q_1^b]$	$\sum_{\vec{x}} \langle \Omega \vert T J_c(x) \bar{J}_c(0) \vert \Omega \rangle$
0^-	$J_c^I = \epsilon_{abc}[q_1^a C q_2^b]$	$\sum_{\vec{x}} \langle \Omega \vert T J_c^I(x) \bar{J}_c^I(0) \vert \Omega \rangle$
0^-	$J_c^0 = \epsilon_{abc}[q_1^a C\gamma_0 q_2^b]$	$\sum_{\vec{x}} \langle \Omega \vert T J_c^0(x) \bar{J}_c^0(0) \vert \Omega \rangle$
1^-	$J_c^{i5} = \epsilon_{abc}[q_1^a C\gamma_i\gamma_5 q_2^b]$	$\frac{1}{3}\sum_i \sum_{\vec{x}} \langle \Omega \vert T J_c^{i5}(x) \bar{J}_c^{i5}(0) \vert \Omega \rangle$

In calculating the two point functions in Table 1, we take a trace in color space and project to zero momentum. Diquarks are not color singlets. Their two point correlation functions have to be computed in a fixed gauge. We use the Landau gauge.

Alternatively, one can combine a diquark with an infinitely heavy quark (i.e. a Polyakov line) to get a color singlet state and calculate its correlation function. This is gauge invariant; however, it may have path dependence [6].

We use the RBC-UKQCD configurations generated with 2+1-flavor domain wall fermions [20]. The parameters of the ensembles used in this work are given in Table 2.

On the coarse lattice, two different light sea quark masses are used to check the sea quark mass dependence of our results. To examine finite lattice spacing effects, we use one ensemble on a fine lattice. To improve the signal, on each configuration on the coarse lattice we compute eight point source quark propagators. The sources are evenly located on eight time slices. On each time slice the source position is randomly chosen from one configuration to another to reduce data correlations. For the vector and axial vector diquarks, we average over the three directions ($i = 1,2,3$) to increase statistics. We also average the data in the forward and backward time directions.

For the valence quark, we use overlap fermions. The massless overlap operator [22] is defined as

$$D_{\rm ov}(\rho) = 1 + \gamma_5 \varepsilon(\gamma_5 D_{\rm w}(\rho)). \tag{1}$$

Here ε is the matrix sign function and $D_{\rm w}(\rho)$ is the usual Wilson fermion operator, except with a negative mass parameter $-\rho = 1/2\kappa - 4$ in which $\kappa_c < \kappa < 0.25$. We use $\kappa = 0.2$ in our calculation, which corresponds to $\rho = 1.5$.

The massive overlap Dirac operator is defined as

$$D_m = \rho D_{\rm ov}(\rho) + m\left(1 - \frac{D_{\rm ov}(\rho)}{2}\right) = \rho + \frac{m}{2} + \left(\rho - \frac{m}{2}\right)\gamma_5\,\varepsilon(\gamma_5 D_{\rm w}(\rho)). \qquad (2)$$

To accommodate the $SU(3)$ chiral transformation, it is usually convenient to use the chirally regulated field $\hat{\psi} = \left(1 - \frac{1}{2}D_{\rm ov}\right)\psi$ in lieu of ψ in the interpolation field and operators. This is equivalent to leaving the unmodified operators and instead adopting the effective quark propagator

$$G \equiv D_{\rm eff}^{-1} \equiv \left(1 - \frac{D_{\rm ov}}{2}\right) D_m^{-1} = \frac{1}{D_c + m}, \qquad (3)$$

where $D_c = \frac{\rho D_{\rm ov}}{1 - D_{\rm ov}/2}$ is chiral, i.e. $\{\gamma_5, D_c\} = 0$ [23].

The overlap valence quark masses in lattice units are given in Table 3. Using the quark mass renormalization constants from Ref. [24] and the lattice spacings, one finds the corresponding $\overline{\rm MS}$ quark masses at 2 GeV are from about 20 MeV to 1 GeV.

The bare quark masses $am_q = 0.067$ and 0.047 on the coarse and fine lattices respectively correspond to the physical strange quark mass within our uncertainty [21]. Our largest quark mass is less than but close to the charm quark mass.

Table 2. Parameters of configurations with 2+1 flavor dynamical domain wall fermions (RBC-UKQCD). The residual masses are from Ref. [20]. The lattice spacings are from Ref. [21].

$1/a$/GeV	label	$am_{\rm sea}$	volume	$N_{\rm src} \times N_{\rm conf}$	$am_{\rm res}$
1.75(4)	c005	0.005/0.04	$24^3 \times 64$	8×92	0.003152(43)
	c02	0.02/0.04	$24^3 \times 64$	8×99	
2.33(5)	f004	0.004/0.03	$32^3 \times 64$	1×50	0.0006664(76)

Table 3. Overlap valence quark masses in lattice units used in this work.

$24^3 \times 64$	0.01350	0.02430	0.04890	0.06700	0.15000	0.33000	0.67000
$32^3 \times 64$	0.00677	0.01290	0.02400	0.04700	0.18000	0.28000	0.50000

3 Results and discussion

In this section, we give the numerical results on all three ensembles given in Table 2. The statistical errors of our results are from bootstraps with 500 samples. On the coarse lattice, we have two ensembles with different light sea quark masses. Thus we only check the sea quark mass dependence in the results but do not try to extrapolate to the chiral limit of the sea quark. The results on the fine lattice, ensemble f004, are used to check the discretization effects but have relatively large uncertainty due to the limited statistics.

3.1 Pion, nucleon and Delta masses

For the convenience of chiral extrapolation later, we first give the pion masses from our data. We also compute the two point correlation functions for the nucleon and Δ^{++} baryon, from which we extract their masses at our pion masses. We use the usual interpolating operators $\bar{u}\gamma_5 d$, $\epsilon_{abc}[u^{Ta}(C\gamma_5)d^b]u^c$ and $\epsilon_{abc}[u^{Ta}(C\gamma_\mu)u^b]u^c$ for these hadrons respectively. The correlation functions are projected to zero 3-momentum and to positive parity (for the baryons). At large t, the ground state dominates and the hadron mass is obtained from a single exponential fit to the correlator.

The numerical values of these hadron masses are given in Tables 4, 5, 6 for ensemble c005, c02 and f004 respectively. On ensemble f004, the signal to noise ratio for the correlators of the Delta baryon is too bad for us to obtain its mass, especially at light quark masses.

Table 4. Pion, nucleon and delta masses from ensemble c005. $1/a = 1.75(4)$ is used to convert to physical units.

$am_{\rm q}$	$am_{\rm ps}$	$m_{\rm ps}$/GeV	$am_{\rm N}$	$am_{\Delta^{++}}$	$a(m_{\Delta^{++}} - m_{\rm N})$
0.01350	0.17911(46)	0.3134(72)	0.677(17)	0.818(41)	0.141(39)
0.02430	0.23670(43)	0.4142(95)	0.7218(61)	0.863(20)	0.141(19)
0.04890	0.33520(55)	0.587(13)	0.8043(64)	0.924(18)	0.120(18)
0.06700	0.39173(46)	0.686(16)	0.8643(47)	0.973(11)	0.109(12)
0.15000	0.60552(35)	1.060(24)	1.1247(42)	1.2049(66)	0.0802(72)
0.33000	0.97666(36)	1.709(39)	1.6398(22)	1.6991(27)	0.0593(26)

At leading order in heavy baryon chiral perturbation theory [25], the nucleon mass is given by

$$M_N = M_0 - 4c_1 m_\pi^2 - \frac{3g_A^2}{32\pi f_\pi^2} m_\pi^3. \tag{4}$$

Here we take the experiment values 1.267 for g_A and 92.4 MeV for f_π to fit our nucleon mass as a function of the pion mass. Note by doing this, we have ignored the effects from the mixed action setup. Half of our pion masses are larger than 600 MeV. Thus we do not expect the pion mass dependence of all the baryon masses can be well described by formulae from chiral perturbation theory. In using Eq.(4) to do the fit, we only include the data points with pion mass less than 600 MeV.

In the left-hand graph of Fig. 1, the nucleon masses from all three ensembles are plotted against the pion mass squared. Here and in the rest of the paper, we have taken into account the uncertainties of the lattice spacings in converting our results into physical units. We do not see big sea quark mass dependence or discretization effects. The two parameter (M_0 and c_1) fit is shown by the red curve and has a χ^2 per degree of freedom (dof) equal to 0.73. At the physical pion mass 140 MeV, the fit gives $m_N = 953(30)$ MeV, which agrees with the experimental value 940 MeV. A three parameter function $M_N = M_0 + c_1 m_\pi^2 + c_2 m_\pi^3$ can also fit the same data with a good χ^2. It gives a nucleon mass (1.09(9) GeV) at the physical point. This is similar to the chiral fits in Refs. [26, 27].

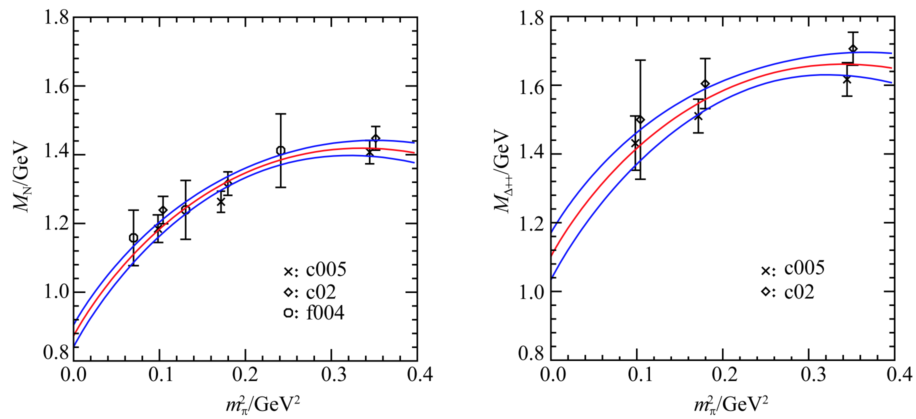

Fig. 1. (color online). Left: The chiral fit to the nucleon mass using data from all three ensembles at pion mass less than 600 MeV. Right: The chiral fit to the mass of Δ^{++} using data from ensembles c005 and c02 at pion masses less than 600 MeV.

For the pion mass dependence of the Delta baryon, the leading one-loop result from heavy baryon chiral perturbation theory has the same form as in Eq.(4) if the $SU(6)$ relation $H_A = 9g_A/5$ is used for the Delta baryon axial coupling H_A. The fit of Eq.(4) to the data points at pion mass less than 600 MeV on ensembles c005 and c02 is shown in the right-hand graph of Fig. 1. The χ^2/dof of the fit is 0.73 and we get $m_\Delta = 1.183(64)$ GeV at the physical pion mass. This should be compared with the experiment value 1232 MeV with a width 117 MeV.

In the last column of Table 4 and Table 5, we give the mass difference between the delta and the nucleon in lattice units. From Eq.(4), we see this mass difference is a linear function of the pion mass squared at leading order. Extrapolating the lowest three data points to the physical pion mass using a linear function of $(am_\pi)^2$, one gets $a(m_{\Delta^{++}} - m_N) = 0.155(32)$ or $m_{\Delta^{++}} - m_N = 272(56)$ MeV for ensemble c005.

Similarly for ensemble c02, we get $a(m_{\Delta^{++}} - m_N) = 0.174(62)$ or $m_{\Delta^{++}} - m_N = 304(108)$ MeV. Both values agree with the experiment value ~ 292 MeV but have large uncertainties.

Table 5. Pion, nucleon and Delta masses from ensemble c02. $1/a = 1.75(4)$ is used to convert to physical units.

am_q	am_{ps}	m_{ps}/GeV	am_N	$am_{\Delta^{++}}$	$a(m_{\Delta^{++}} - m_N)$
0.01350	0.18440(63)	0.3227(75)	0.708(16)	0.857(97)	0.149(95)
0.02430	0.24213(53)	0.4237(97)	0.7520(91)	0.917(36)	0.165(35)
0.04890	0.33899(56)	0.593(14)	0.8272(56)	0.975(16)	0.148(20)
0.06700	0.39692(55)	0.695(16)	0.8936(41)	1.0313(94)	0.138(12)
0.15000	0.60939(47)	1.066(24)	1.1622(28)	1.2584(51)	0.0962(57)
0.33000	0.98015(30)	1.715(39)	1.6594(23)	1.7196(33)	0.0602(40)

Table 6. Pion and nucleon masses from ensemble f004. $1/a = 2.33(5)$ is used to convert to physical units.

$am_{\rm q}$	$am_{\rm ps}$	$m_{\rm ps}$/GeV	$am_{\rm N}$
0.00677	0.1134(35)	0.2642(99)	0.497(33)
0.01290	0.1550(26)	0.3612(98)	0.532(35)
0.02400	0.2106(15)	0.491(11)	0.606(44)
0.04700	0.2970(10)	0.692(15)	0.672(12)
0.18000	0.6321(10)	1.473(32)	1.0848(72)
0.28000	0.8394(11)	1.956(42)	1.3851(44)

3.2 Quark correlation functions

The diquark-quark mass difference is a measure of the strength of the diquark correlation. This difference for the good diquark is estimated from hadron spectrum in Ref. [16]. We obtain the quark mass from the scalar part of the quark propagator $S(x,0)$ in the Landau gauge

$$C_{\rm q}(t) = \sum_{\vec{x}} S_{ii}^{aa}(x,0), \tag{5}$$

where the color index a and spin index i are summed over. A single exponential fit (actually a hyperbolic sine function because of the boundary condition in the time direction) taking into account data correlations to $C_{\rm q}(t)$ at large t, for example $t \in [13,28]$, gives the quark mass $aM_{\rm q}$ at each bare valence quark mass. Examples of the effective mass $\ln(C_{\rm q}(t)/C_{\rm q}(t+1))$ and the results from the exponential fits are shown in Fig. 2.

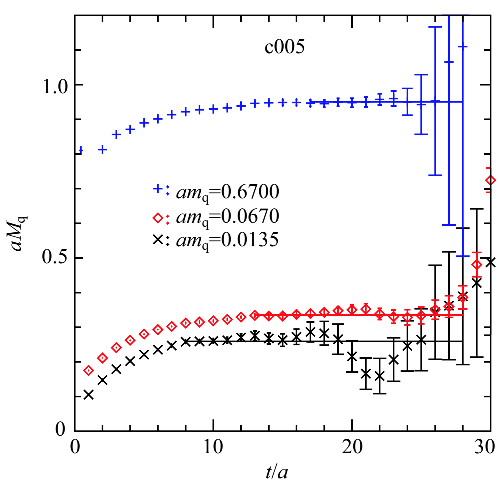

Fig. 2. (color online). The effective quark mass $\ln(C_{\rm q}(t)/C_{\rm q}(t+1))$ at various bare valence quark masses for ensemble c005 with sea quark masses $m_l/m_s = 0.005/0.04$. The straight lines mark the results of the quark mass from single exponential fits to the correlators $C_{\rm q}(t)$. The fitting ranges of t are also indicated by the lines.

The quark masses $aM_{\rm q}$ are collected in Table 7 for all three ensembles.

Table 7. Quark masses for various valence quark masses on all three ensembles. The first line is a linear extrapolation in $am_{\rm q}$ to the chiral limit with the lowest four quark masses.

$am_{\rm q}$(coarse)	$aM_{\rm q}$(c005)	$aM_{\rm q}$(c02)	$am_{\rm q}$(fine)	$aM_{\rm q}$(f004)
0.0	0.2361(44)	0.2813(86)	0.0	0.1832(99)
0.01350	0.2592(47)	0.298(12)	0.00677	0.196(14)
0.02430	0.2695(35)	0.3034(73)	0.01290	0.199(10)
0.04890	0.3102(46)	0.3258(43)	0.02400	0.2144(89)
0.06700	0.3351(45)	0.3443(37)	0.04700	0.2466(81)
0.15000	0.4282(30)	0.4362(32)	0.18000	0.3893(79)
0.33000	0.6190(57)	0.6264(58)	0.28000	0.5006(92)
0.67000	0.9504(85)	0.9559(88)	0.50000	0.721(12)

They are plotted against the bare quark mass for ensemble c005 in Fig. 3.

With a linear fit to the lightest four quark masses (the corresponding current quark masses are not heavier than the physical strange quark mass), one finds in the chiral limit $aM_{\rm q} = 0.2361(44)$ or $M_{\rm q} = 413(12)$ MeV by using $1/a = 1.75(4)$ GeV. The fitting is also shown in Fig. 3 by the red line.

Similarly on the ensemble c02, we obtain $aM_{\rm q} = 0.2813(86)$ or $M_{\rm q} = 492(19)$ MeV in the chiral limit by a linear extrapolation with the lowest four quark masses. The two ensembles c02 and c005 have different sea quark masses. To see the sea quark mass dependence more clearly, we plot $aM_{\rm q}$ from the two ensembles together in Fig. 4. We see that there is a clear sea quark mass dependence in our results when the valence quark mass is less than the physical strange quark mass ($am_{\rm q} \leqslant 0.067$). The quark mass $aM_{\rm q}$ from the scalar part of the quark propagator in Landau gauge decreases as the sea quark mass decreases.

The results from ensemble f004 are also given in Table 7. In the chiral limit of the valence quark mass, we get $aM_{\rm q} = 0.1832(99)$ or $M_{\rm q} = 427(25)$ MeV by using $1/a = 2.33(5)$ GeV. If using the lowest five data points to do the linear extrapolation, then we find $aM_{\rm q} = 0.1889(58)$ or $M_{\rm q} = 440(16)$ MeV. The light sea quark mass for ensemble f004 is lighter than but close to that for c005. Since the number $M_{\rm q} = 427(25)$ MeV agrees with the result 413(12) MeV from c005, we do not see apparent discretization effects in $M_{\rm q}$ with our statistical uncertainty.

Although the quark mass $M_{\rm q}$ here is in principle gauge dependent, it was shown this dependence may be small in covariant gauges including the Landau gauge [28]. If we average the quark masses $M_{\rm q}$ from c005 and f004 using the inverse of their squared error as the weight, then we obtain $M_{\rm q} = 416(11)$ MeV. Here the inverse of the square of the final statistical uncertainty is equal to the sum of the inverse squared error (the weight). Note our sea quark mass is still larger than the physical one. $M_{\rm q}$ is in general consistent with constituent quark masses (350–400 MeV) used in various models.

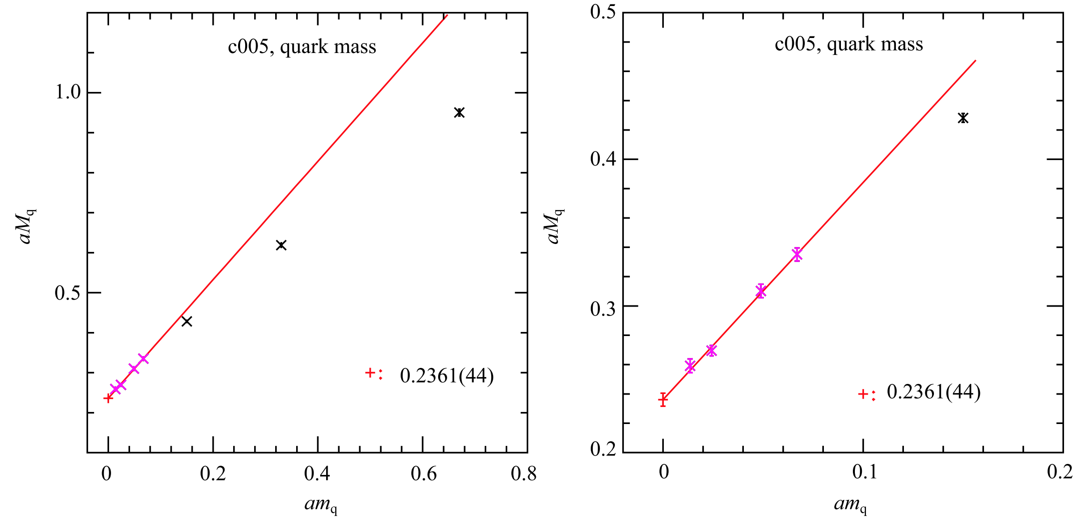

Fig. 3. (color online). Quark masses aM_{q} against the bare valence quark mass am_{q} for ensemble c005 with sea quark masses $m_{\mathrm{l}}/m_{\mathrm{s}} = 0.005/0.04$. The straight line is a linear fit to the lightest four quark masses. The graph on the right is a zoom in of the left.

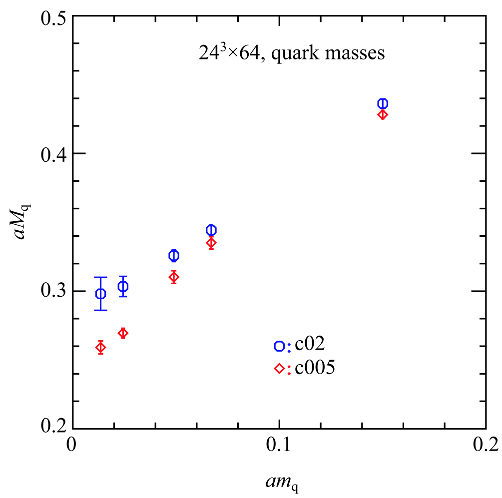

Fig. 4. (color online). Quark masses from the scalar part of quark propagators against the bare valence quark masses on the two coarse lattices with different sea quark masses.

For the strange quark, its bare valence quark mass is roughly 0.067 and 0.047 on the coarse and fine lattice respectively [21]. The corresponding quark mass M_s from the scalar part of the quark propagator is 586(16), 603(15) and 575(23) MeV on the three ensembles c005, c02 and f004 respectively (see Table 7). Unlike the light quark mass M_q, the sea quark mass dependence in M_s is much smaller.

3.3 Diquark masses and mass differences

3.3.1 Diquarks composed of two light quarks

We start with diquarks composed of the up and down quarks, i.e. $q_1 = u$ and $q_2 = d$ in Table 1. The two point functions of the diquarks exhibit an exponential decay behaviour similar to that of ordinary hadron correlation functions. This can be clearly seen in the effective mass plot shown by Fig. 5 from the correlation functions using J_c^5 and J_c^{05}.

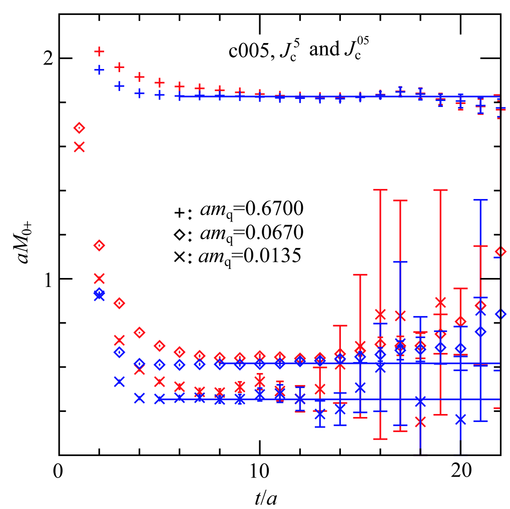

Fig. 5. (color online). Effective scalar diquark masses at various valence quark masses on ensemble c005 with sea quark masses $m_l/m_s = 0.005/0.04$. The red symbols are from the correlators from J_c^5. The blue ones are from J_c^{05}. The straight lines mark the results of the scalar diquark mass from single exponential fits to the correlation functions using J_c^{05}. The fitting ranges of t are indicated by the length of the lines.

Both currents J_c^5 and J_c^{05} can give us the scalar diquark mass. The effective masses from the two currents go to the same plateau at large t as we see in the graph, but the plateau for J_c^{05} appears earlier than that for J_c^5. Therefore we fit the correlators from J_c^{05} to determine the scalar diquark mass. In Fig. 5 the lines indicate the results from single exponential fittings to the correlators at different quark masses.

The numerical results of the scalar diquark mass are given in Table 8 for c005. With a linear chiral extrapolation, the scalar diquark mass from J_c^{05} is 725(20) MeV by using $1/a = 1.75(4)$ GeV.

Then the scalar diquark and quark mass difference from ensemble c005 is $725(20) - 413(12) = 312(23)$ MeV. Here the final uncertainty is from a simple error propagation. This number is in good agreement with the estimation ~ 310 MeV in Ref. [16].

The results from ensemble c02 are obtained similarly and are collected in Table 9.

In the chiral limit, the scalar diquark mass from ensemble c02 is 797(24) MeV by using $1/a = 1.75(4)$ GeV. This value is a little different from 725(20) MeV for ensemble c005. Thus there seems to be some sea quark mass dependence in the absolute value of the scalar diquark mass. The scalar diquark and quark mass difference is $797(24) - 492(19) = 305(31)$ MeV, which agrees with the result 312(23) MeV from ensemble c005. Therefore we do not see sea quark mass dependence in the diquark quark mass difference.

Table 8. Diquark masses and mass difference for various valence quark masses on ensemble c005. The first line is a linear extrapolation in $am_{\rm q}$ to the chiral limit with the lowest four data points.

$am_{\rm q}$	$aM_{0^+}(J_c^{05})$	$aM_{1^+}(J_c^i)$	$a(M_{1^+} - M_{0^+})$	$aM_{0^-}(J_c^I)$	aM_{1^-}
0.0	0.4142(63)	0.584(21)	0.166(22)	-	-
0.01350	0.4534(70)	0.611(29)	0.158(31)	-	-
0.02430	0.4875(52)	0.635(18)	0.148(19)	0.796(52)	-
0.04890	0.5692(37)	0.694(10)	0.1248(98)	0.862(23)	0.987(53)
0.06700	0.6166(48)	0.7300(85)	0.1134(93)	0.904(18)	1.003(41)
0.15000	0.8293(70)	0.8907(68)	0.0614(89)	1.056(29)	1.140(24)
0.33000	1.1830(30)	1.2334(55)	0.0504(45)	1.378(17)	1.454(21)
0.67000	1.8265(39)	1.8604(68)	0.0339(62)	1.976(12)	2.025(16)

Table 9. Diquark masses and mass difference for various valence quark masses on ensemble c02. The first line is a linear extrapolation in $am_{\rm q}$ to the chiral limit with the lowest four data points.

$am_{\rm q}$	$aM_{0^+}(J_c^{05})$	$aM_{1^+}(J_c^i)$	$a(M_{1^+} - M_{0^+})$	$aM_{0^-}(J_c^I)$	aM_{1^-}
0.0	0.4555(91)	0.644(16)	0.185(20)	-	-
0.01350	0.491(10)	0.662(21)	0.171(26)	-	-
0.02430	0.5256(80)	0.687(13)	0.161(16)	0.900(57)	-
0.04890	0.5998(75)	0.727(11)	0.127(12)	0.950(22)	0.956(79)
0.06700	0.6453(63)	0.7574(85)	0.1121(95)	0.984(16)	1.011(64)
0.15000	0.8521(76)	0.9145(58)	0.0624(87)	1.104(13)	1.165(33)
0.33000	1.2060(56)	1.2459(56)	0.0399(53)	1.400(19)	1.441(25)
0.67000	1.836(11)	1.8588(94)	0.0228(77)	1.969(14)	2.053(16)

Table 10. Diquark masses and mass difference for various valence quark masses on ensemble f004. The first line is a linear extrapolation in $am_{\rm q}$ to the chiral limit with the lowest four data points.

$am_{\rm q}$	$aM_{0^+}(J_c^{05})$	$aM_{1^+}(J_c^i)$	$a(M_{1^+} - M_{0^+})$	$aM_{0^-}(J_c^I)$	aM_{1^-}
0.0	0.296(19)	0.425(24)	0.128(30)	-	-
0.00677	0.318(28)	0.438(46)	0.120(54)	-	-
0.01290	0.340(22)	0.460(24)	0.120(32)	-	-
0.02400	0.379(15)	0.487(18)	0.108(23)	-	-
0.04700	0.457(10)	0.547(15)	0.090(18)	0.61(10)	0.565(17)
0.18000	0.7879(84)	0.835(11)	0.047(13)	0.957(20)	0.829(19)
0.28000	0.9977(84)	1.031(10)	0.033(11)	1.136(26)	1.017(13)
0.50000	1.4299(90)	1.447(14)	0.017(15)	1.592(16)	1.454(15)

The results on the fine lattice f004 are given in Table 10. The scalar diquark mass in the chiral limit is $aM_{0^+} = 0.296(19)$ or $M_{0^+} = 690(47)$ MeV. With a relatively large error, it is in agreement with the number 725(20) MeV from ensemble c005, which indicates the finite lattice spacing effect is smaller than our statistical uncertainty. The mass difference between the scalar diquark and the light quark is $690(47)-427(25)=263(53)$ MeV. It just agrees with the results 312(23) MeV and 305(31) MeV from c005 and c02 respectively.

We average the scalar diquark and quark mass difference from the three ensembles using the inverse of their squared error as the weight. The sum of the inverse squared error gives the inverse of the final uncertainty squared. In this way, we obtain $M_{0^+} - M_q = 304(17)$ MeV, where the error is statistical (including the uncertainties of lattice spacing).

The mass of the bad diquark can be extracted from the correlators using J_c^i or J_c. The fitting results by using a single exponential from the two currents are in agreement. However, the signal of the correlator from J_c^i is better. Therefore we collect the bad diquark masses from this current in Table 8 for c005. A linear extrapolation to the chiral limit with the lowest four data points gives $aM_{1^+} = 0.584(21)$ or $M_{1^+} = 1022(44)$ MeV.

The bad and good diquark mass difference (in lattice units) is plotted against the valence quark mass in Fig. 6. Here the uncertainties are from bootstrap analysis. As we can see, the difference decreases as the quark mass increases.

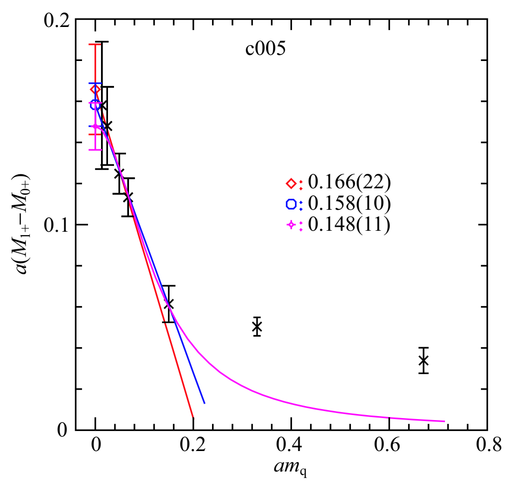

Fig. 6. (color online). The mass difference between bad and good diquarks as a function of the valence quark mass on ensemble c005. The diquarks are composed of two degenerate light quarks. The red straight line is a linear extrapolation in am_q to the chiral limit using the lowest four data points. The blue straight line uses the lowest five data points. The magenta curve is the fit using Eq.(6) to the lowest five points.

The simplest chiral extrapolation of the mass difference is a straight line fit. Using the lowest four data points, one gets $a(M_{1^+} - M_{0^+}) = 0.166(22)$ or $M_{1^+} - M_{0^+} = 291(39)$ MeV. If we use the lowest five data points for the linear chiral extrapolation, then we get $a(M_{1^+} - M_{0^+}) = 0.158(10)$, which agrees with the result by using the lowest four data points.

We also tried an ansatz similar to the one used in Ref. [7]. Diquark correlations come from spin dependent forces. The bad and good diquark mass difference Δm is expected to scale like $1/(m_{q_1}m_{q_2})$ at large quark mass [16]. In the chiral limit, the mass difference goes to a constant. Thus one can try the following ansatz for diquarks composed of two degenerate quarks

$$\Delta m = \frac{a_1}{1+a_2 m_q^2}, \tag{6}$$

where a_1 and a_2 are two fitting parameters. We find that this ansatz cannot fit all seven data points with an acceptable χ^2/dof. If we limit to the lowest five data points, we can get a χ^2/dof<1 and find $a(M_{1^+}-M_{0^+}) = 0.148(11)$. The fit is shown by the curve in Fig. 6.

For the bad diquark from ensemble c02, a linear extrapolation to the chiral limit with the lowest four data points gives $aM_{1^+} = 0.644(16)$, which is higher than 0.584(21) from ensemble c005. The bad and scalar diquark mass difference is given in the fourth column of Table 9. Unlike the absolute value of diquark masses, the diquark mass differences on the two ensembles are in agreement within statistical uncertainties. In the left graph of Fig. 7, the mass differences are plotted against the valence quark mass from ensembles c005 and c02. It does not show apparent sea quark mass dependence.

On ensemble f004, the bad diquark mass in the chiral limit is $aM_{1^+} = 0.425(24)$ or $M_{1^+} = 990(60)$ MeV, which is in agreement with the result 1022(44) MeV from c005. Therefore we do not see discretization effects with our current statistical uncertainties. The fourth column in Table 10 is the bad and good diquark mass difference on the fine lattice.

We plot the bad and good diquark mass difference in physical units against the pion mass squared on all three ensembles in the right graph of Fig. 7. All lattice results seem to lie on a universal curve, which means sea quark mass dependence and discretization effects are small compared with the statistical errors. By using the lowest order relation $m_\pi^2 \propto m_q$, Eq.(6) can be written as

$$\Delta m = \frac{b_1}{1+b_2 m_\pi^4}. \tag{7}$$

This ansatz can fit the data points at $m_\pi^2 < 1.2(0.6)$ GeV^2 and gives $M_{1^+} - M_{0^+} = 264(14)(285(20))$ MeV (χ^2/dof=3.2/12(1.2/10)). Alternatively, a linear extrapolation in m_π^2 with the data points at $m_\pi^2 < 1.2(0.6)$ GeV^2

gives $M_{1^+} - M_{0^+} = 280(12)(309(25))$ MeV. The average of the four center values is 285 MeV. Taking the largest statistical error and the largest change in the center value as the systematic error, we get $M_{1^+} - M_{0^+} = 285(25)(45)$ MeV. This number is a little bigger than the estimation ~ 210 MeV in Ref. [16], which used masses of baryons with a strange or charm quark.

For the diquark with quantum number $J^P = 0^-$, we tried two interpolating operators J_c^{I} and J_c^0. The correlators from both operators are noisy with the one from J_c^{I} having a better signal. The masses from single exponential fits to the correlators of J_c^{I} on ensemble c005, c02 and f004 are given in Tables 8, 9, 10 respectively. Examples of the effective mass plateau are shown in the left graph of Fig. 8.

At some of the small valence quark masses, no result is obtained due to the bad signal to noise ratio. These results confirm that the 0^- diquark is heavier than both the 0^+ and 1^+ diquarks.

The correlator for the vector diquark is even noisier. The extracted diquark masses are listed in Table 8 and Table 9 for the two ensembles on the coarse lattice respectively. The right graph in Fig. 8 shows two examples of the effective mass for this channel. The vector diquark seems to be heavier than the 0^- diquark. But with our statistical uncertainty, it is hard to determine. On ensemble f004 (see Table 10), the 0^- diquark seems to be heavier than the vector diquark. More statistics are needed to improve the mass plateaus for the 0^- and 1^- diquarks.

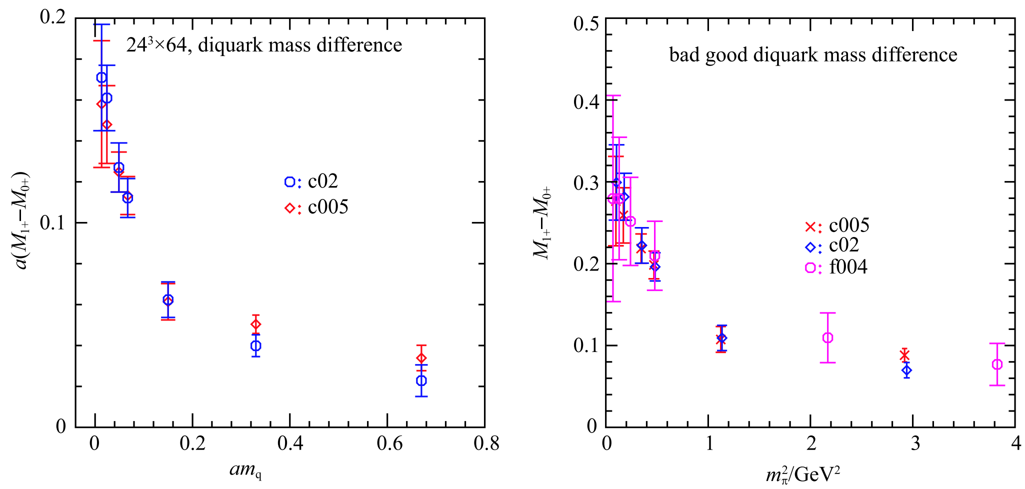

Fig. 7. (color online). Left: The mass difference between bad and good diquarks as a function of the valence quark mass on ensemble c005 and c02. The results from the two ensembles are in agreement, which means the mass difference has small sea quark mass dependence. Right: The mass difference (GeV) against the pion mass squared on all three ensembles.

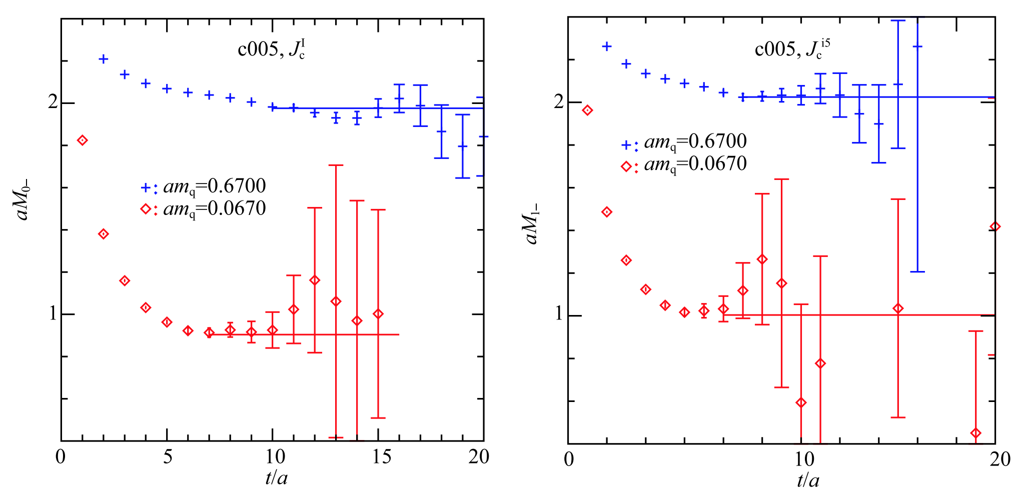

Fig. 8. (color online). Effective masses of the 0^- (left) and 1^- (right) diquarks at two valence quark masses on ensemble c005. The 0^- diquark uses correlators from J_c^{I}. The straight lines mark the diquark mass from single exponential fits to the correlation functions. The fitting ranges of t are indicated by the length of the lines.

3.3.2 Diquarks with a strange and a light quark

Now we turn to diquarks composed of a strange and a light quark. We set $q_1 = u$ and $q_2 = s$ in the currents given in Table 1. Therefore we use $am_{q_2} = 0.0670$ and $am_{q_1} = 0.0135$, 0.0243, 0.0489, 0.0670 on the coarse lattice. The scalar and bad diquark masses together with their difference are given in Tables 11, 12 as we vary the mass of q_1 on the two ensembles c005 and c02.

Table 11. Diquark masses and mass difference for various light quark masses on ensemble c005. The diquarks are composed of a strange and a light quark. The first line is a linear extrapolation in am_{q_1} to the chiral limit.

am_{q_1}	$aM_{0^+}(J_c^{05})$	$aM_{1^+}(J_c^i)$	$a(M_{1^+} - M_{0^+})$
0.0	0.5177(43)	0.609(16)	-
0.01350	0.5376(42)	0.633(18)	0.095(18)
0.02430	0.5534(38)	0.656(14)	0.103(15)
0.04890	0.5884(32)	0.691(10)	0.103(11)
0.06700	0.6166(48)	0.7300(85)	0.1134(93)

Table 12. Diquark masses and mass difference for various light quark masses on ensemble c02. The diquarks are composed of a strange and a light quark. The first line is a linear extrapolation in am_{q_1} to the chiral limit.

am_{q_1}	$aM_{0^+}(J_c^{05})$	$aM_{1^+}(J_c^i)$	$a(M_{1^+} - M_{0^+})$
0.0	0.579(13)	0.6883(86)	-
0.01350	0.593(14)	0.7037(89)	0.111(17)
0.02430	0.602(12)	0.7119(72)	0.110(14)
0.04890	0.629(10)	0.7337(60)	0.105(12)
0.06700	0.6453(63)	0.7574(85)	0.1121(95)

In the chiral limit of the up quark, we obtain $aM_{0^+} = 0.5177(43)$ by doing a linear extrapolation in am_{q_1} on ensemble c005. In physical units, it is 906(22) MeV. For the scalar diquark and strange quark mass difference, one gets $0.5177(43) - 0.3351(45) = 0.1826(62)$ in lattice units or 320(13) MeV, which is of the same size as 312(23) MeV for the scalar diquark composed of two light quarks. On ensemble c02, this difference is $0.579(13) - 0.3443(37) = 0.235(14)$ or 411(26) MeV. It is heavier than the result on c005, showing some sea quark mass dependence. This dependence mainly comes from the scalar diquark mass since the strange quark mass M_s is not so sensitive to the light sea quark mass (see the end of Sec. 3.2).

On the fine lattice, we set $am_{q_2} = 0.04700$ and $am_{q_1} = 0.00677$, 0.01290, 0.02400, 0.04700. In Table 13, we give the diquark masses from ensemble f004.

The scalar diquark and strange quark mass difference is $0.3862(93) - 0.2466(81) = 0.140(12)$ or 326(29) MeV. This agrees with the result 320(13) MeV from c005, indicating a small discretization effect in this difference. Averaging the results from c005 and f004 weighted by their inverse squared error, one gets $M_{0^+} - M_s = 321(12)$ MeV for diquarks composed of a light and a strange quark.

Table 13. Diquark masses and mass difference for various light quark masses on ensemble f004. The diquarks are composed of a strange and a light quark. The first line is a linear extrapolation in am_{q_1} to the chiral limit.

am_{q_1}	$aM_{0^+}(J_c^{05})$	$aM_{1^+}(J_c^i)$	$a(M_{1^+} - M_{0^+})$
0.0	0.3862(93)	0.453(14)	-
0.00677	0.395(11)	0.466(16)	0.071(19)
0.01290	0.406(10)	0.481(15)	0.075(17)
0.02400	0.4246(97)	0.497(13)	0.072(17)
0.04700	0.457(10)	0.547(15)	0.090(18)

Using the results 320 MeV and 411 MeV from c005 and c02 respectively, we can do a linear extrapolation to the light sea quark massless limit: $a(m_{\rm sea} + m_{\rm res}) = 0$. What we get is 271(49) MeV. Taking the difference between 320 MeV and 271 MeV as a systematic error, we find $M_{0^+} - M_s = 321(12)(49)$ MeV. This number is smaller than the estimation ~ 500 MeV in Ref. [16].

For the bad diquark mass, we also do a linear extrapolation in the light valence quark mass and find 0.609(16) in the chiral limit (1.066(37) MeV in physical units) on c005. Using this number and the chiral limit value of the good diquark mass 0.5177(43), one gets the mass difference in the chiral limit as 0.091(17) or 159(30) MeV. It agrees with the estimation of this diquark mass difference (152 MeV) in Ref. [16] obtained from baryon masses in the charm sector. Compared with the case for diquarks composed of two light quarks, this difference decreases as one of the light quarks is changed to a strange quark.

On ensemble c02, the absolute values of the bad and good diquark masses seem heavier than their counterparts on ensemble c005, indicating some sea quark mass dependence. This is similar to the case for diquarks composed of two light quarks. The mass difference between the bad and good diquarks on ensemble c02 agrees with that on ensemble c005, showing that the sea quark mass dependence is smaller in the difference than in the absolute diquark masses.

On ensemble f004, the scalar and bad diquark masses in the chiral limit of m_{q_1} are 900(29) MeV and 1.055(40) MeV respectively. Both are in agreement with their counterparts from c005. Thus discretization effects are again shown to be small.

The scalar and bad diquark mass difference from all three ensembles are plotted in Fig. 9 as a function of the squared mass of the pion composed of light quark q_1 (see Tables 4, 5, 6).

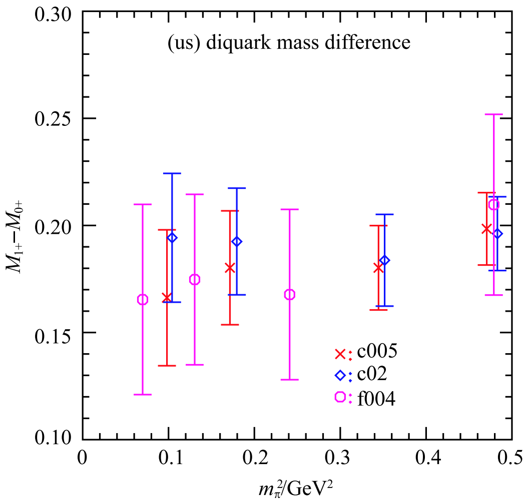

Fig. 9. (color online). The scalar and bad diquark mass difference (GeV) against the pion mass squared on all three ensembles. The diquarks are composed of a strange and a light quark.

As we can see from the graph, the dependence of the mass difference on the light quark mass (or pion mass) seems small with our current statistical uncertainty. One can fit the difference either with a straight line in m_π^2 or with a constant. The straight line fit gives $M_{1^+}-M_{0^+}=171(18)$ MeV. The constant fit gives $M_{1^+}-M_{0^+}=188(7)$ MeV. Averaging the two, we get 180(18)(17) MeV. Here the first uncertainty is the bigger of the two statistical errors and the second is the systematic error from the change in the central values.

4 Summary

Using overlap valence quarks on configurations with 2+1 flavors of domain wall sea quarks, we calculated the mass and mass difference of various diquarks in the Landau gauge. We also calculated the diquark quark mass difference. We extrapolate the results to the valence quark chiral limit and check the sea quark mass dependence using two ensembles with the same coarse lattice spacing. Discretization effects are examined by working on a fine lattice.

The scalar diquark has the lowest mass which means it is the channel with the strongest correlation. The mass difference between the axial vector and scalar diquark (composed of two light quarks) decreases as the valence quark mass increases. This was also observed in previous lattice calculations [6–8].

We see sea quark mass dependence in the absolute values of diquark and quark masses. Their masses decrease as the sea quark mass decreases. This dependence is small (smaller than our statistical error) in diquark mass difference and diquark quark mass difference. For the diquark composed of a strange and a light quark, the mass difference between the scalar diquark and the strange quark shows some sea quark mass dependence. From our data we do not expect this difference to increase as the light sea quark mass lowers to the physical value. Within our limited statistics on the fine lattice, we do not see apparent discretization effects in any of our results.

Our final results of the mass differences are given in Table 14.

Table 14. Diquark mass difference and diquark quark mass difference (MeV). The diquarks are either composed of two light quarks or composed of a strange and a light quark. The first (or the only) error is statistical and the second (when there is one) is a systematic error.

(ud)	$M_{0+}-M_q$	$M_{1+}-M_{0+}$
this work	304(17)	285(25)(45)
[16]	∼310	∼210
(us)	$M_{0+}-M_s$	$M_{1+}-M_{0+}$
this work	321(12)(49)	180(18)(17)
[16]	∼500	∼150

In the chiral limit of the valence quark mass, we find the diquark mass difference $M_{1^+}-M_{0^+}=285(25)(45)$ MeV and diquark quark mass difference $M_{0^+}-M_{\rm q}=304(17)$ MeV for diquarks composed of two light quarks. For diquarks composed of a strange and a light quark, we obtain $M_{1^+}-M_{0^+}=180(18)(17)$ MeV and $M_{0^+}-M_{\rm s}=321(12)(49)$ MeV. Here when there are two uncertainties, the first is statistical and the second is a systematic error estimated from different extrapolations to the chiral limit or from light sea quark mass dependence. In general, the results of these mass differences agree with the estimations from hadron spectroscopy in Ref. [16]. The exception is $M_{0^+}-M_{\rm s}=321(12)(49)$ MeV for the scalar diquark composed of a strange and an up quark, which is smaller than the estimation ~ 500 MeV in Ref. [16].

To better control the light sea quark mass dependence and finite lattice spacing effects in our work, calculations at another sea quark mass are needed, and more statistics on the fine lattice should be added. It might be interesting to calculate these differences in other gauges to check the gauge dependence.

We thank the RBC-UKQCD collaboration for sharing the domain wall fermion configurations. Parts of the fittings were done by using Meinel's public code [29].

References

1 M. Anselmino, E. Predazzi, S. Ekelin, S. Fredriksson, and D. B. Lichtenberg, Rev. Mod. Phys., **65**: 1199 (1993)
2 H. G. Dosch, M. Jamin, and B. Stech, Z. Phys. C, **42**: 167 (1989)
3 M. Neubert, and B. Stech, Phys. Rev. D, **44**: 775 (1991)
4 S. K. Choi et al (Belle Collaboration), Phys. Rev. Lett., **91**: 262001 (2003)
5 K. A. Olive et al (Particle Data Group Collaboration), Chin. Phys. C, **38**: 090001 (2014)
6 M. Hess, F. Karsch, E. Laermann, and I. Wetzorke, Phys. Rev. D, **58**: 111502 (1998)
7 C. Alexandrou, Ph. de Forcrand, and B. Lucini, Phys. Rev. Lett., **97**: 222002 (2006)
8 R. Babich, N. Garron, C. Hoelbling, J. Howard, L. Lellouch, and C. Rebbi, Phys. Rev. D, **76**: 074021 (2007)
9 K. Orginos, PoS LAT2005: 054 (2006)
10 Z. Fodor, C. Hoelbling, M. Mechtel, and K. Szabo, PoS LAT2005: 310 (2006)
11 T. DeGrand, Z. Liu, and S. Schaefer, Phys. Rev. D, **77**: 034505 (2008)
12 J. Green, J. Negele, M. Engelhardt, and P. Varilly, PoS LATTICE **2010**: 140 (2010)
13 R. T. Kleiv, T. G. Steele, A. Zhang, and I. Blokland, Phys. Rev. D, **87** (12): 125018 (2013)
14 Z. G. Wang, Commun. Theor. Phys., **59**: 451 (2013)
15 L. Tang and X. Q. Li, Chin. Phys. C, **36**: 578 (2012)
16 R. L. Jaffe, Phys. Rept., **409**: 1 (2005)
17 T. A. DeGrand, R. L. Jaffe, K. Johnson, and J. E. Kiskis, Phys. Rev. D, **12**: 2060 (1975).
18 G. 't Hooft, Phys. Rev. D, **14**: 3432 (1976); Phys. Rev. D, **18**: 2199 (1978)
19 T. Schäfer and E. V. Shuryak, Rev. Mod. Phys., **70**: 323 (1998)
20 Y. Aoki et al (RBC and UKQCD Collaborations), Phys. Rev. D, **83**: 074508 (2011)
21 Y. B. Yang et al, Phys. Rev. D, **92** (3): 034517 (2015)
22 H. Neuberger, Phys. Lett. B, **417**: 141 (1998)
23 T. W. Chiu and S. V. Zenkin, Phys. Rev. D, **59**: 074501 (1999)
24 Z. Liu et al (chiQCD Collaboration), Phys. Rev. D, **90** (3): 034505 (2014)
25 J. Gasser, M. E. Sainio and A. Svarc, Nucl. Phys. B, **307**: 779 (1988)
26 M. Gong et al (XQCD Collaboration), Phys. Rev. D, **88**: 014503 (2013)
27 K. F. Liu, Y. Chen, M. Gong, R. Sufian, M. Sun, and A. Li, PoS LATTICE **2013**: 507 (2014)
28 C. W. Bernard, D. Murphy, A. Soni, and K. K. Yee, Nucl. Phys. Proc. Suppl., **17**: 593 (1990)
29 Available from http://www.stefanmeinel.com/software/